

Influence of Field-Dependent Critical Current on Harmonic AC Loss Analysis in HTS Coils for Superconducting Transformers Supplying Non-Linear Loads

Mohammad Yazdani-Asrami, S. Asghar Gholamian, Seyyed Mehdi Mirimani, and Jafar Adabi

Abstract— There are two main obstacles in front of the development of high temperature superconducting (HTS) conductors for electrical power network applications; tape price and cooling cost. In order to reduce cooling cost, it is vital to evaluate AC transport current loss of the tapes precisely and then reduce it by some design innovations. In addition, AC transport current loss in HTS materials is a critical design variable for large-scale power network applications such as HTS transformers, superconducting fault current limiters, and power cables, since they are continuously carrying the network/load current during their operating life. In existing power network, harmonic production sources are commonly used and thus, currents are distorted. Therefore, the effect of nonsinusoidal current on the critical apparatus in the network such as transformer must be studied. In this paper, AC transport current loss of a single-turn 2G YBCO HTS coil has been modelled and numerically calculated under nonsinusoidal transport current using finite element method. Furthermore, influence of dependency of critical current density to magnetic field on the AC transport current loss of HTS coil when carries distorted currents has been considered. It has been observed that nonsinusoidal current causes excessive losses in HTS coil. On the other hand, a case study on an HTS transformer supplying non-linear load with harmonic currents has been considered to study the loss increment as well as heat load change. It is been observed that current harmonics increases the AC loss, and heat load of transformer and decreases the efficiency, consequently.

Index Terms— AC transport current loss, Electrical power network, Finite element method, Harmonic distortion, Heat load estimation, HTS coil, HTS power transformer, Non-linear load.

I. INTRODUCTION

SECOND generation (2G) high temperature superconducting (HTS) YBCO tapes are the most desired candidates to be implemented in fabrication of superconducting apparatus for electrical network applications, especially HTS transformers, HTS power cables, and superconducting fault current limiters (SFCLs). These devices are particularly attractive to manufacturers and power network utilities for their great advantages such as very low load loss, high efficiency and high current density compared to the conventional devices, which for example leads to fabrication of a compact HTS transformer with small occupied space and light weight which are premium benefits compared with same-class conventional transformers. Since large-scale power applications of HTS technology such as HTS transformer or SFCLs involves HTS winding and normally needs high carrying current density, so, HTS wires or tapes are normally employed to wind coil [1-8].

In power network applications, the AC current passes through HTS coil and produces an AC magnetic flux which dissipate some energy in the coil as AC transport current loss. The energy dissipation in the HTS coil has significant impact on the optimal and economical design of superconducting network apparatus such as HTS transformer as the most important power grid equipments. The knowledge of correct estimation of AC transport current loss leads to approaches to interpret the physical/magnetic mechanisms of the loss production, investigate loss mitigation procedures for the HTS coils at transformer design level, and help to design a reliable and appropriate cryogenic system. It is because, due to AC loss increase, the cryocooler heat load increases and as a result, overall efficiency decreases and finally leads to a more complex design process [6-12].

Among different ways to evaluate the AC transport current loss of an HTS coil or tape, experimental approaches are expensive, risky, and sometimes destructive, while analytical methods are accurate enough but limited to simple geometry or problems. The numerical modelling is an essential approach for the preliminary design of practical HTS power transformers

M. Yazdani-Asrami, is with Department of Electronic & Electrical Engineering, University of Strathclyde, Glasgow, G1 1XW, UK. (e-mail: m.yazdaniasrami@gmail.com).

S. A. Gholamian, S. M. Mirimani, and J. Adabi are with Department of Electrical and Computer Engineering, Babol Noshirvani University of Technology, Babol, Iran.

because with ever-increasing development of multiphysical simulation softwares, modelling is generally simple, low cost, without any destruction risk of any equipment or superconductor. For AC transport loss calculation, the accurate distribution of current density as well as calculation of electric and magnetic field inside the superconductor is essential [13-17].

The published research works in the literature have been mainly focused on the AC transport current loss for low power and frequency applications with sinusoidal excitation [18-23]. While the current in the power network which pass through HTS transformers or SFCLs are no longer sinusoidal because of the widespread of the switching transients, non-linear loads, and power electronic devices in grid [24-28]; then it is essential for HTS power applications to estimate the effect of nonsinusoidal currents on the AC loss, precisely. For this purpose, several theoretical studies have been done in order to analytically calculate the AC loss under nonsinusoidal current. In [29-31], authors tried to derive a rather simple and straightforward closed form equation based on harmonic orders to calculate the AC transport losses of the HTS tapes. In [32], the AC losses in racetrack coil which is made by YBCO tapes have been measured for nonsinusoidal transport currents with fundamental frequencies up to 1 kHz. In this paper, highly polluted nonsinusoidal current with trapezoidal and triangular shapes were considered which cannot be the good representative of the harmonic distortion in the power network for HTS transformer study. In [33-34], AC losses of pancake HTS coil under four different waveform excitations (saw-tooth, triangle, sinusoidal and square) were measured to investigate effect of the input current amplitude and its frequency on losses. While the currents are all out of sinusoidal shape but normally transformers never face with such distorted currents in power networks. In [35], AC loss of HTS stack under distorted currents have been calculated for SFCL applications. In [36], authors characterized the nonsinusoidal AC loss of three commonly used HTS coils in superconducting machines, i.e. double-pancake, single-pancake, and helical coils. The AC losses generated by 3rd, and 5th harmonic orders were studied, to demonstrate how different harmonics change the AC loss profile versus harmonic content.

In this paper, AC transport current losses of a single-turn HTS coil subjected to nonsinusoidal current were numerically calculated at different carrying current levels, frequencies, and total harmonic distortions (THDs) using two-dimensional (2D) axisymmetric finite element (FE) method in COMSOL Multiphysics software package. The effect of B-dependent critical current density on the AC loss results was investigated precisely. Then, the results were compared with the AC transport current loss of sinusoidal current at the same current level and frequencies. A series of case studies have been simulated in order to investigate the effect of different THDs on the AC transport current loss. As authors focused on the HTS transformer application in this paper, the most significant harmonic orders of in current of a polluted power network i.e. the 5th and 7th harmonics were considered in case study simulations. Finally, influence of nonsinusoidal current with combination of several harmonic orders were studied on the AC loss and heat load of a 20 MVA superconducting power transformer. Authors shown that how behavior of combined harmonic orders as a spectrum is different from when they were applied independently to HTS coil.

The rest of paper has been organized as follow, section II contains modelling procedure and FE H-formulation method, and section III contains simulation results for case studies of the AC transport current loss of HTS coil and some discussions on the results, and section IV contains the results of AC loss calculation on HTS power transformers, and section V contains summaries and conclusions.

II. FINITE ELEMENT MODELLING OF AC TRANSPORT CURRENT LOSS IN HTS COIL

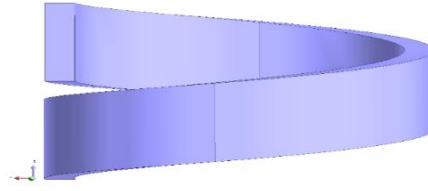
In this section, FE modelling of AC transport current loss for a single-turn HTS coil made by a coated conductor has been explained using H-formulation. Since, the HTS tapes in the coils/windings of an HTS transformer or SFCL are always immobilized on a non-magnetic non-conductive former in vertical position, therefore 2D axisymmetric modelling has been done. In Fig.1, the coil schematic was shown in 2D and 3D views in order to help to imagine the geometry easier.

A. Overview of FE method

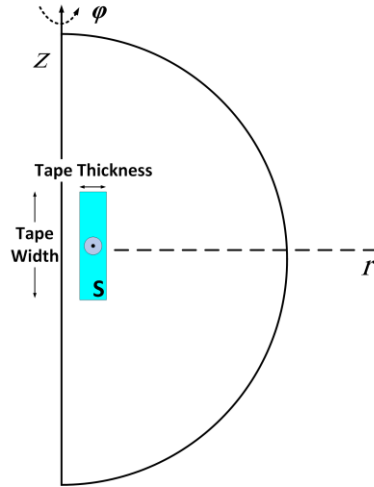
FE-based softwares are vastly used as sophisticated tools by many engineers and scientists in order to solve multiphysical problems such as electromagnetic, thermal, and fluid flow in last two decades, especially in design stage. The FE method is strictly the most superior numerical method for simulating physical field distributions in electrical machine studies. The FE method finds the solution to any engineering problem that can be formulated by a finite set of spatial partial derivative equations with appropriate boundary and initial conditions. It is widely used to solve problems for static, steady-state and transient engineering applications in electrical engineering [37].

In power transformer studies, FE method solves the electromagnetic field problems by solving Maxwell equations in a finite region of space with appropriate boundary conditions and user-specified initial conditions in order to obtain a solution with guaranteed uniqueness and precision. In order to obtain the set of equations to solve, the geometry of the problem would be discretized automatically into many small elements. The assembly of small element is referred to as the finite element mesh of the model or simply the mesh. In regions with rapid spatial field variation, the mesh density needs to be increased for better accuracy [24, 37]. Furthermore, the structured mapped mesh makes the convergence faster in simulation of HTS

components [38].



(a) 3D Schematic of a single-turn coil.



(b) 2D view of the cross section in the study with applied current

Fig. 1. Different 3D and 2D views of a single-turn coil in the study

B. Overview of different methods for AC transport current loss modelling

When an HTS coil is subjected to AC excitation, the cyclic or transient magnetic field interacts with the HTS material leads to energy dissipation in coil. If the magnetic field is only self-generated field, the AC loss would be AC transport current loss at self-field [39]. This AC loss generating components are divide into two main categories [15-17, 39-42]: 1) Hysteresis loss which is caused by the penetration and movement of the magnetic flux in the HTS material. 2) Eddy current loss which is caused by the currents induced by a magnetic field and circulating in the normal metal parts of HTS conductor. It should be mentioned that sometimes the tape has ferromagnetic substrate, thus, ferromagnetic loss in this layer should be added to other components of loss in superconducting coil.

The FE modelling methods for calculating AC loss of HTS conductors were divided into four major formulation systems in the literature [15-18, 39-42]: 1) the A-V formulation which solves magnetic vector potential (A), 2) the T- Ω which solves current vector potential (T), 3) the E formulation, 4) the magnetic field (H) formulation which directly solves the magnetic field.

These formulations are derived from Maxwell equations but based on different state variables. The selection of appropriate model parameters is vital to ensure a proper solving time and good convergence. The H-formulation method is of interest because of excellent convergence, simplicity of imposing boundary conditions, and no need to add artificial small resistivity in E-J equation which has been used to avoid singularity problem in other methods. The H-formulation is implemented with edge element functions to solve Maxwell equations. The magnetic field H is solved in the time domain which is different from a succession of critical state solutions and then the relaxation effects in the magnetic field inside the HTS material are taken into account. The nonlinearities are treated by a classical Newton method that minimizes the residual of the linearized equations under a certain threshold at each time step before moving on to the next time step [15-18, 40-43].

C. H-formulation for FE modelling of AC transport current loss in single-turn HTS coil

In order to study the electromagnetic behavior of a single-turn HTS coil, the H-formulation is implemented as a sophisticated FE modelling approach, which is able to compute the hysteresis and eddy current losses of HTS coil, precisely. Since the modelling has been done for 2D axisymmetric environment, thus $\mathbf{H} = [H_r, H_z]$.

The H-formulations for FE modelling of a typical HTS single-turn coil are as follows [33-35]:

Faraday's law:

$$\nabla \times \mathbf{E} = -\frac{\partial \mathbf{B}}{\partial t} \quad (1)$$

Ampere's law:

$$\nabla \times \mathbf{H} = \mathbf{J} \quad (2)$$

Ohm's law:

$$\mathbf{E} = \rho \mathbf{J} \quad (3)$$

Constitutive law:

$$\mathbf{B} = \mu_0 \mu_r \mathbf{H} \quad (4)$$

Where, \mathbf{E} is the electric field, \mathbf{B} is the magnetic flux density, \mathbf{H} is the magnetic field intensity, \mathbf{J} is the current density, ρ is the resistivity, μ_0 is the permeability of free space, and μ_r is the relative permeability.

The E-J power law without dependency of critical current density to magnetic field (B-independent critical current density):

$$\frac{E}{J} = \left(\frac{E_0}{J_{c0}} \right) \left(\left| \frac{J}{J_{c0}} \right| \right)^{n-1} \quad (5)$$

Equation (5) is the general E-J power law for HTS modelling, where E_0 is the characteristic electric field equal to $1 \mu\text{V}\cdot\text{cm}^{-1}$, J_{c0} is the critical current density in the self-field at 77 K, J_c is the critical current density and n is the power factor constant of I-V characteristic which is usually between 20 to 30 for existing commercial tapes.

The in-field performance of critical current density is the most important characteristic for modelling of an HTS coil in any practical applications, especially for superconducting power transformers. The E-J power law with B-dependent critical current density which can take overcritical current densities into account, is shown based on equations (6) and (7):

$$\frac{E}{J} = \left(\frac{E_0}{J_c} \right) \left(\left| \frac{J}{J_c} \right| \right)^{n-1} \quad (6)$$

$$J_c = \left(\frac{J_{c0}}{1 + \frac{|B|}{B_0}} \right) \quad (7)$$

$$\rho_{HTS}(\mathbf{J}, \mathbf{B}) = \left(\frac{E_0}{J_{c0}} \right) \left(1 + \frac{|B|}{B_0} \right) \left(\left| \frac{J}{J_{c0}} \right| \right)^{n-1} \quad (8)$$

The equations (6) and (7), express B-dependent E-J power law for considering dependency of critical current density to magnetic field in modelling of HTS coil, where B_0 is the field dependency factor.

The general form of partial differential equation (PDE) which would be computed by COMSOL Multiphysics is as follows:

$$\frac{\partial(\mu_0 \mu_r \mathbf{H})}{\partial t} + \nabla \times (\rho \nabla \times \mathbf{H}) = 0 \quad (9)$$

The global constraint of general PDE have been performed to inject the desired transport current into the HTS coil. The magnitude of the transport current I_{exc} has been given by the integration of the current density \mathbf{J} on the HTS domain, S :

$$\mathbf{I}_{exc} = \int_S \mathbf{J} \, d\mathbf{S} \quad (10)$$

To impose an unequivocal transport current in the conductor, integral constraints are used, so that the total carrying current can be arbitrarily specified using a nonsinusoidal current as function of time. For this purpose, Neumann boundary condition has been applied to the single-turn HTS coil.

The AC transport current loss (P_{loss}) of the domain S can be calculated as follows:

$$\mathbf{P}_{loss} = \mathbf{Q} = 2 f \int_{T/2}^T \int_S \mathbf{E} \cdot \mathbf{J} \, d\mathbf{S} \, dt \quad (11)$$

Where f and T are frequency and the period of one cycle of transport current.

III. CASE STUDIES: SIMULATION RESULTS AND DISCUSSION

In order to study the frequency and magnetic field dependence of different loss components, a series of H-formulations FE simulations have been conducted on a typical HTS coil with the real dimensions of HTS layer, substrate, and stabilizer. For this purpose, some case studies on single-turn coil were simulated in COMSOL Multiphysics using a personal computer with the following settings: Intel Core i7-5500U 2.4 GHz CPU 8GB RAM.

The flowchart for the modeling of single-turn HTS coil when carries nonsinusoidal current, and the process to calculate its AC transport current loss have been illustrated in Fig.2. The specifications of the single-turn HTS coil have been tabulated in Table I.

A. AC Transport current loss calculation under sinusoidal excitation

In order to calculate the AC transport current loss of the single-turn HTS coil, the 2D FE model were implemented in COMSOL Multiphysics based on Fig.2. For this purpose, 2D axisymmetric FE modelling were used to draw geometries of the coil and region. The radius of the circular region is ten times bigger than the external radius of the HTS coil. The structured mapped mesh has been used for superconducting area and the rest of the model meshed by fine triangular meshes. The mesh configuration of the modelling region and single-turn HTS coil in COMSOL Multiphysics environment were shown in different views in Fig.3.

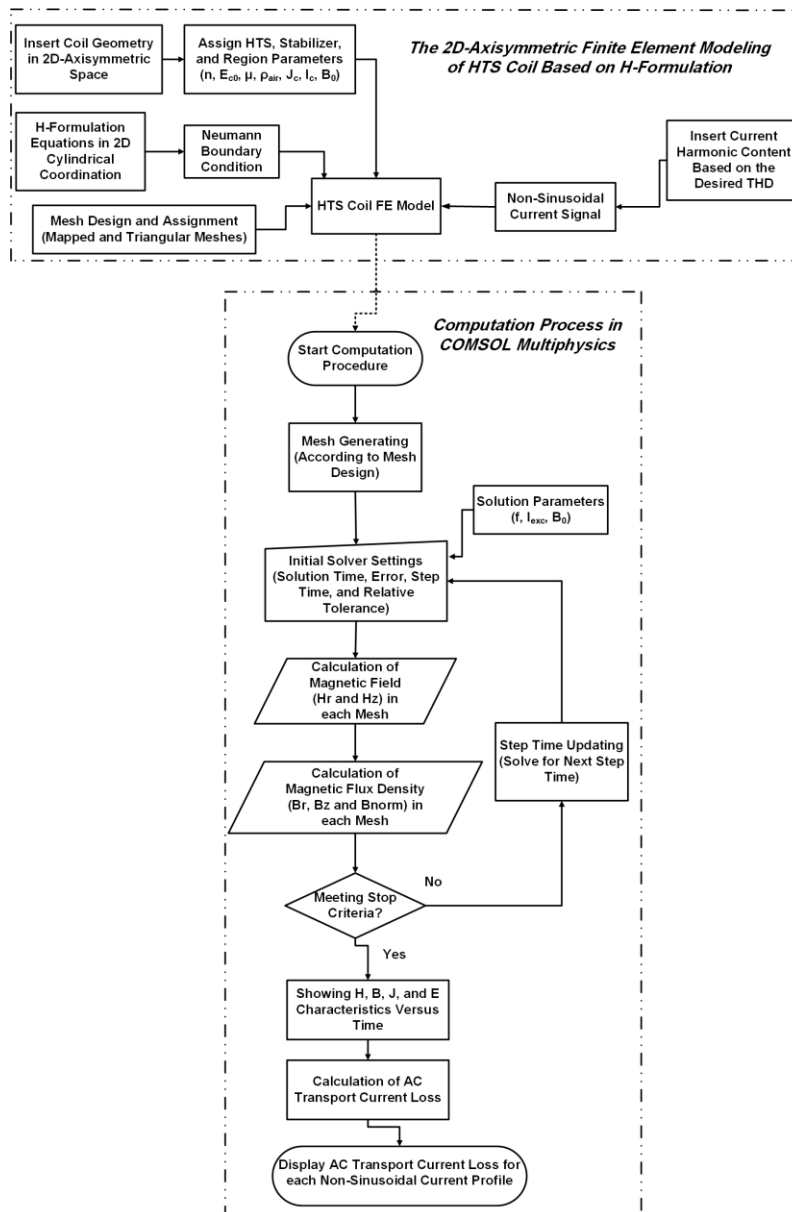


Fig. 2. The flowchart for FE modeling of single-turn HTS coil in order to compute the AC transport current loss under nonsinusoidal carrying current

TABLE I
THE SPECIFICATIONS OF HTS COIL FOR FE SIMULATIONS

Parameter	Quantity	Dimension
Thickness of HTS layer (tsc)	1	μm
Width of tape (wsc)	4	mm
Critical current (I_c) @ 77K	86	A
E-J power law factor (n)	30	---
Characteristic electric field (E_0) @ 77K	1	$\mu\text{V}\cdot\text{cm}^{-1}$
Internal diameter of coil former (R_i)	50	mm
Coil former coil		Fiber-glass

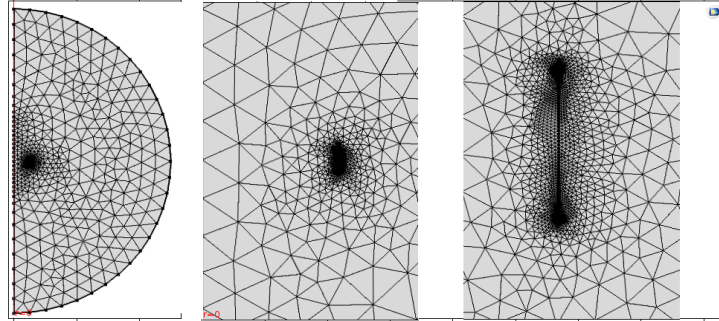


Fig. 3. The mesh operation on the model

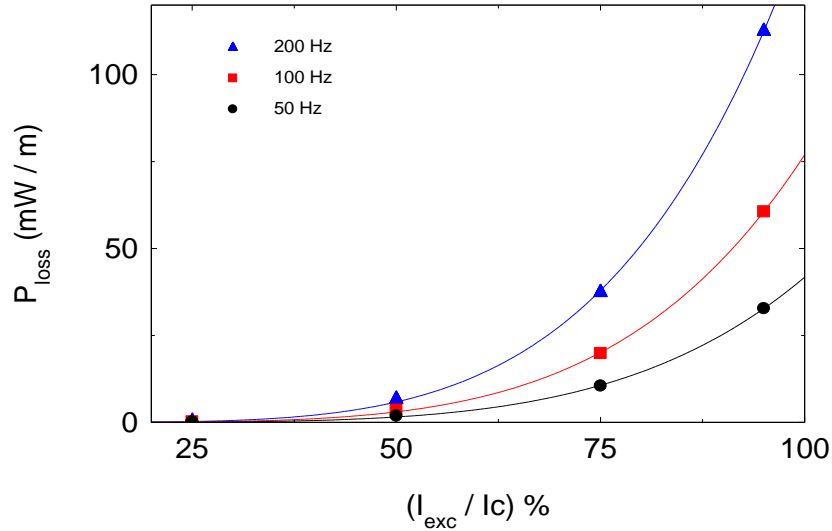


Fig. 4. The calculated AC transport current losses of HTS coil for different sinusoidal current and frequency levels

In order to study the AC transport current loss of the single-turn HTS coil under sinusoidal excitation, the carrying currents at 25%, 50%, 75%, and 95% of the critical current were applied to the coil at 50, 100 and 200 Hz in COMSOL Multiphysics. At first, equation (5) has been used to define the relation between E and J. The calculated AC transport current loss for different carrying current and frequency levels were shown in Fig.4. With frequency increase, AC loss increases drastically. But more interestingly the AC loss versus carrying current increases with power law which have been shown on Fig.4 at different frequency levels.

The dependency of critical current density of the coil to magnetic field must be considered in order to calculate AC transport loss, accurately. For this purpose, equation (6) to (8) were applied to the FE model of the HTS coil. In Fig.5, effect of dependency of critical current density to magnetic field on the calculated AC transport current losses at different sinusoidal carrying current and frequency levels were illustrated in logarithmic scales when B_0 is equal to 125 mT. It should be mentioned that the leakage magnetic field in a power transformer is in the range of 70 to 150 mT.

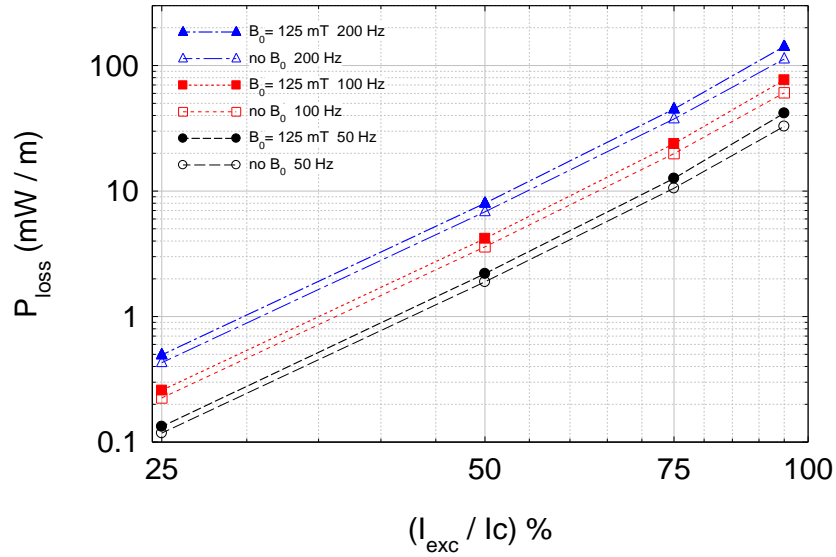


Fig. 5. The effect of dependency of critical current density to magnetic field on the calculated AC transport current losses of modeled HTS coil for different sinusoidal transport current and frequencies in logarithmic scales

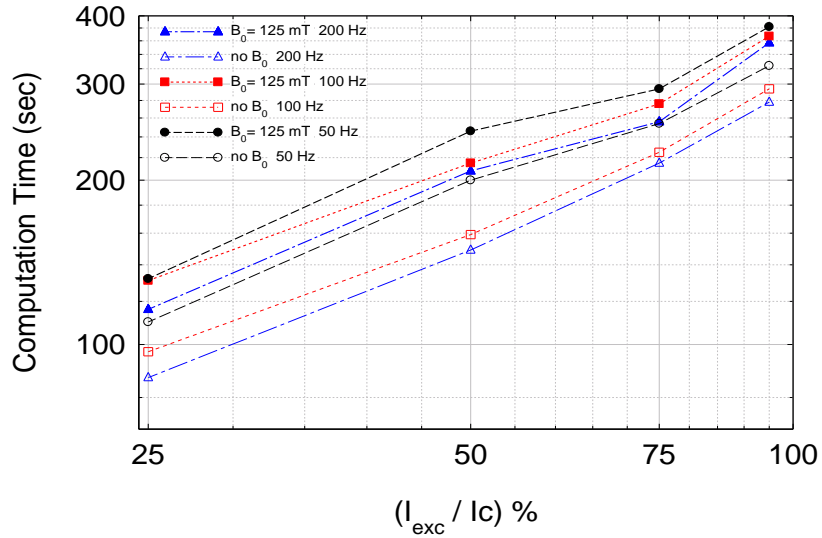


Fig. 6. The computation time for a cycle of carrying current at different sinusoidal transport current and frequency levels in logarithmic scales at two different B-dependency level

The calculated AC transport current loss increases when B-dependent critical current density was considered in simulations; because J_c decreases by changing B_0 from infinity to 125 mT and also, the resistivity of HTS material increases. The relative increase of AC transport current loss for two B_0 -independent and B_0 -dependent current densities versus carrying current shows a constant increase for different frequency levels. The average of this relative increase versus carrying current at different fraction of critical current were shown in Table 2. These average numbers can be considered as a kind of error in simulation when depend of J_c to B is not considered; because the content of Table II shows without consideration of B-dependency of the critical current density, the estimated loss is 15% to 25% lower than B-dependent values which represents the real situation.

The comparison of computation time between B-dependent and B-independent simulations for a full cycle of a sinusoidal transport current at different conditions (amplitude and frequency) were shown in Fig.6 in logarithmic scales. When current density is B-independent, computation time versus transport current increases almost with a power law and in higher frequency the computation is faster. When current density has considered as B-dependent leads to a slower solving process, and computation time increases by 20% to 40% compared with B-independent modelling case. In addition, when transport current increase from quarter of the critical current to almost close to critical current, computation time of the simulations increases about 3 times for a constant frequency. Also, if an average computation time be calculated for a specific transport current level, then, the average increase of computation time versus transport current is 20% to 30% higher when critical current density is B-dependent.

TABLE II
AVERAGE RELATIVE INCREASE OF AC TRANSPORT CURRENT LOSS DUE TO B-DEPENDENT CRITICAL CURRENT

(I_{exc}/I_c) (%)	$Average \left\{ \left(\frac{P_{loss}(125 \text{ mT}) - P_{loss}(B_{independent})}{P_{loss}(B_{independent})} \right) \times 100 \right\}$
25	14.45
50	16.64
75	19.84
95	26.56

TABLE III
THE HARMONIC CONTENTS OF NONSINUSOIDAL CURRENTS FOR EXCITING STUDIED HTS COIL

Case No.	$\left(\frac{h_5}{h_1}\right)$ %	THD (%)	Relative Amplitude Increase (%)
1	5	5	0.125
2	10	10	0.5
3	15	15	1.19
4	20	20	1.98

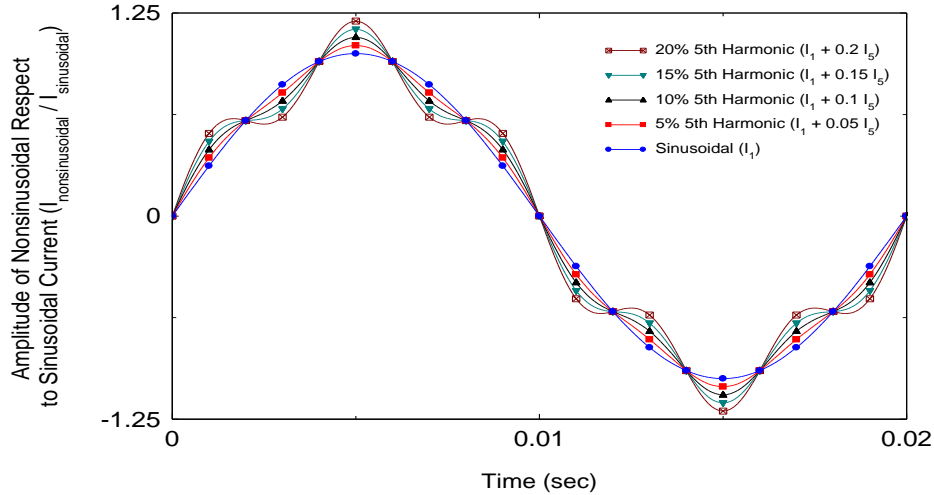


Fig. 7. The distorted current waveforms

B. AC Transport current loss calculation under nonsinusoidal excitation

In this section, the effect of nonsinusoidal excitation on the AC transport current loss of HTS coil were investigated. For this purpose, 5th harmonic component was added to the sinusoidal waveform in order to obtain the distorted current. The harmonic content of the distorted currents – as case studies - were tabulated in Table III. In addition, the effect of these harmonic components on the distortion of the sinusoidal current waveform was illustrated in Fig.7. It should be mentioned that the THDs of the applied transport current were chosen to model both low and high distortion level in current which cover different kinds and sources of current distortions for power transformers in electrical power networks in both distribution and transmission levels.

Relative Amplitude Increase (RAI) which is mentioned in Table III was calculated as follows:

$$RAI\% = (h_1 - \sqrt{h_1^2 + h_5^2}) \times 100 \quad (12)$$

The difference between RAI and THD is very important to focus. The THD only explains how the current waveform is distorted and far away from pure sinusoidal one, but the RAI explains how amplitude increased respect to sinusoidal current. The AC loss would increase because of both of them. For example, in case no.4, THD of 5th harmonic is 20% which means the amplitude of the 5th order harmonic is 20% of fundamental harmonic, while the value of RAI is less than 2%. Thus, while current waveform is significantly distorted and out of sinusoidal waveform, but the amplitude of distorted current has only

increased 2% more than sinusoidal one.

The simulation of case studies for the single-turn HTS coil were done in COMSOL Multiphysics when carries nonsinusoidal transport current with nominal magnitude of 25%, 50%, 75%, and 95% of critical current. The fundamental frequency of applied nonsinusoidal carrying currents have been considered as 200 Hz to make the simulation process faster. In addition, all the case studies were simulated for two cases; B-independent and B-dependent J_c with $B_0=125$ mT.

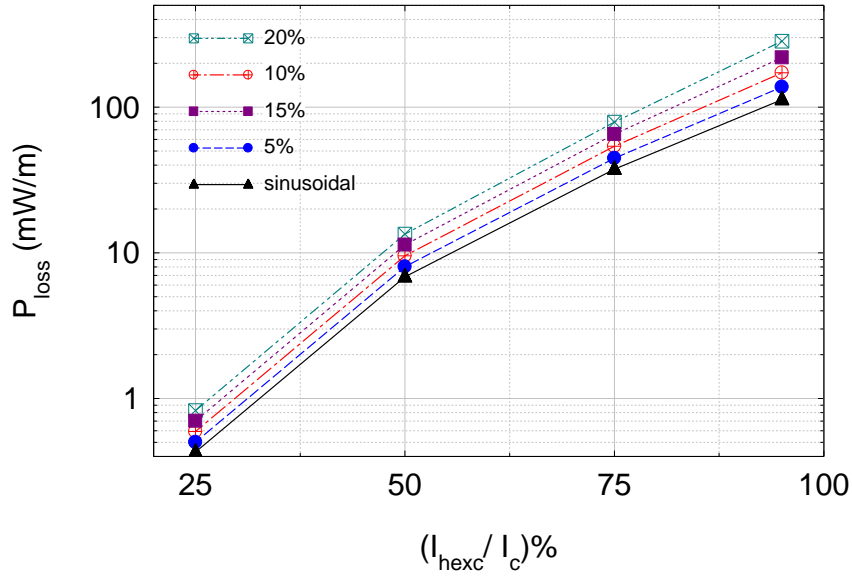


Fig. 8. The variation of the calculated AC transport current losses of modeled HTS coil for different sinusoidal and nonsinusoidal transport current at different THDs with B-independent current density in logarithmic scales

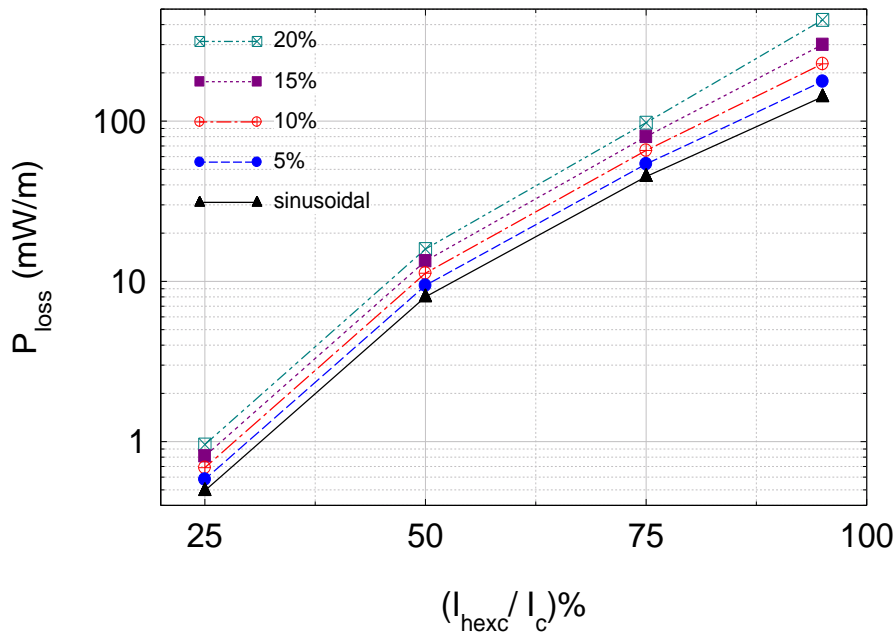


Fig. 9. The variation of the calculated AC transport current losses of modeled HTS coil for different sinusoidal and nonsinusoidal transport current at different THDs with B-dependent current density at B_0 equal to 125 mT in logarithmic scales

In Fig.8 and Fig.9, the calculated AC transport current losses of the HTS coil for different sinusoidal and nonsinusoidal carrying current with different THDs were shown in logarithmic scales with B-independent and B-dependent ($B_0 = 125$ mT) current density, respectively. It can be concluded from Fig.8 and Fig.9 that by increasing the amplitude of nonsinusoidal carrying current, the AC transport current loss increases, drastically, and this increase is proportional to THD of the applied current. Since both Fig.8 and Fig.9 were illustrated in logarithmic scale, it can be seen, by 4 times increase of the carrying current, AC transport current loss multiplies more than 400 times. The loss increment is higher when B-dependent J_c was

considered in the model. Another issue to focus on is that when HTS coil carries a transport current near critical current, any possible intense harmonic distortion can get the HTS material to overload situation and a region between superconducting and metallic phases. This phenomenon is very dangerous when the HTS coil is utilized in HTS transformer winding. Therefore, HTS transformer design must consider such an effect during design process.

The loss increases with THD of nonsinusoidal carrying current. This increase is not linear and the relative loss increase changes at different transport current level. Fig.10 shows the variation of AC transport current loss of HTS coil versus the 5th harmonic content of carrying current. The AC loss is higher when the model is B-dependent J_c with B₀ = 125 mT compared with B-independent case. The slope of the AC loss curves at different carrying current levels in Fig.10 are not equals. The higher carrying currents have a bigger slope. In addition, the relative AC transport current loss increment versus THD of nonsinusoidal current were calculated from Fig.10 and were shown in Fig.11. The variation of relative increase of AC transport current loss versus THD shows that the slope of the curves increases very fast with THD. The slope trends of the depicted curves in Fig.11 are perfectly matched with a power law fit as follow:

$$\text{Relative Increase} = a \times (\text{THD})^b + c \quad (13)$$

Where *a* is the slope of linear part of the curve, *b* is power law factor and *c* is the related AC transport loss at sinusoidal carrying current. After curve fitting, the power law factors are extracted from the fits which are tabulated in Table IV. Thus, it is obvious from content of Table IV that, in higher current level which are close to critical current of the coil, the AC transport current loss increases very fast because there is a big jump in *b* factor at 95% carrying current from 1.5 to 2.1. It is because the tape in the coil would go to the flux flow region, and AC loss increases accordingly.

TABLE IV
THE POWER FACTOR (B COEFFICIENT OF EQUATION 13) OF THE CURVE FITTINGS FOR RELATIVE INCREASE OF AC TRANSPORT CURRENT LOSS

(I _{exc} /I _c) (%)	B-independent Model	B-dependent Model B ₀ =125 mT
25	1.38	1.4
50	1.39	1.42
75	1.46	1.5
95	1.73	2.1

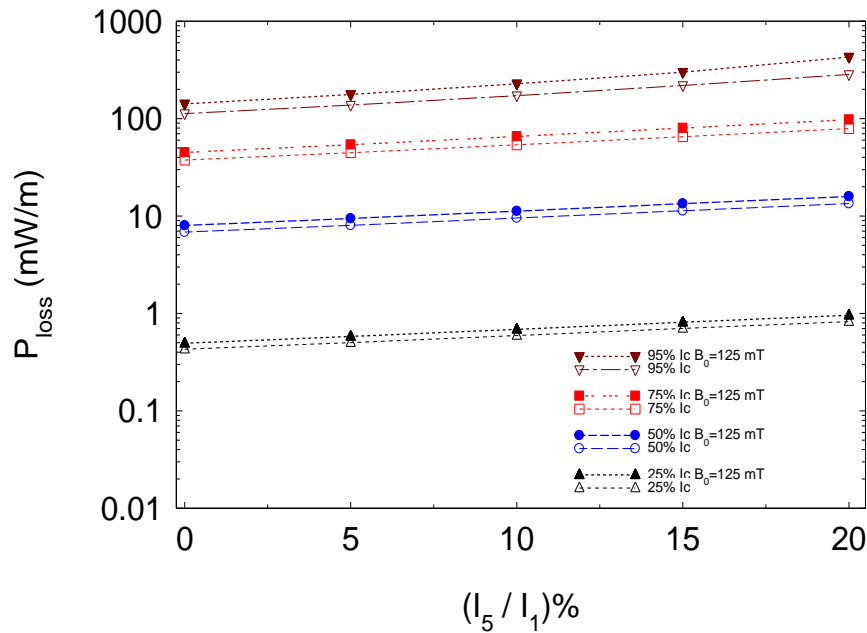


Fig. 10. Effect of B-dependency of J_c on the value of AC transport current losses of HTS coil at different THDs and nonsinusoidal carrying current levels

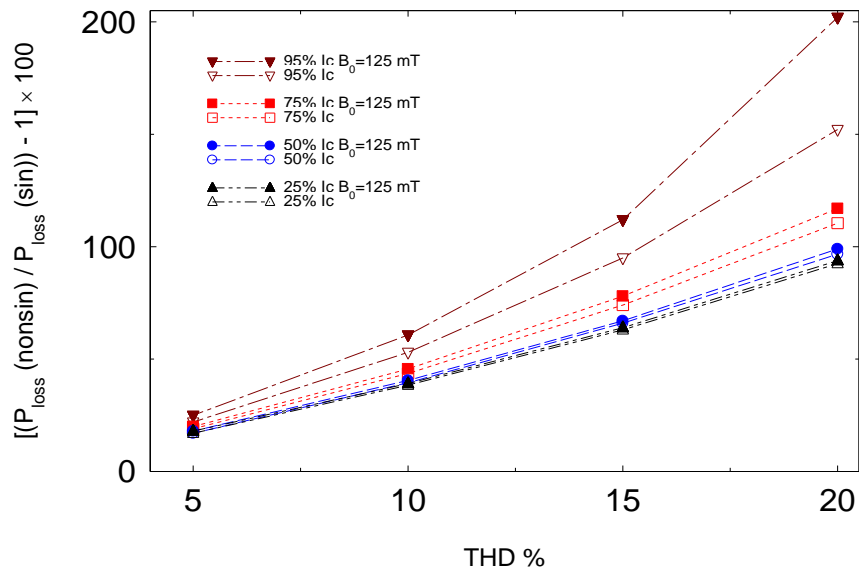


Fig. 11. Relative increase of AC transport current loss of HTS coil versus different THD of nonsinusoidal carrying current considering B-dependent J_c model

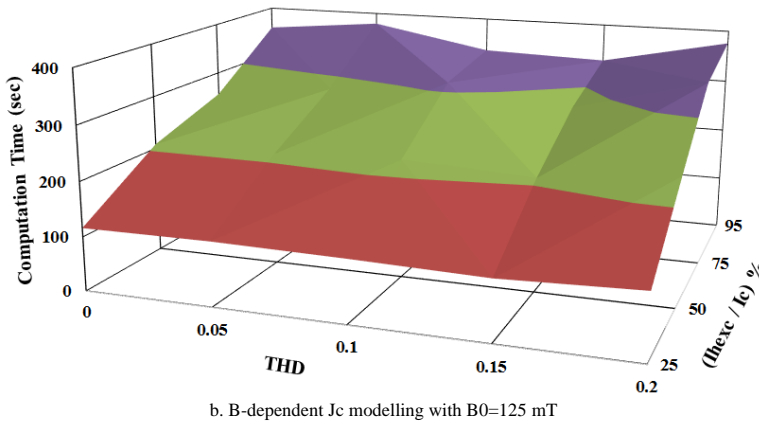
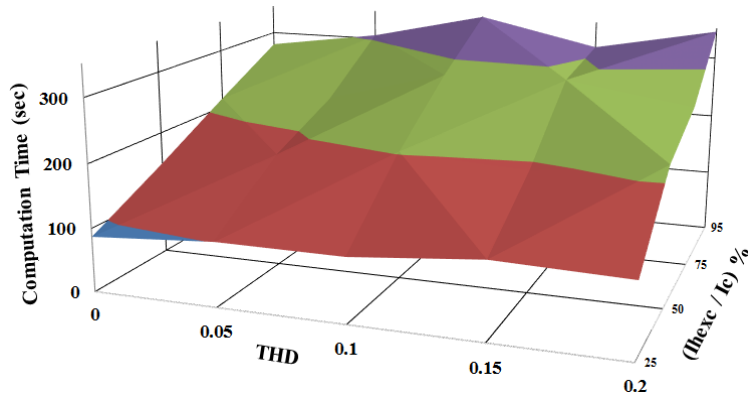


Fig. 12. The 3D plains to show computation time of simulations for AC transport current loss calculations of HTS coil versus different THDs at different nonsinusoidal carrying current levels

In numerical modelling of HTS coils under nonsinusoidal currents, the computation time is very important to choose the proper modelling method. The computation time in a simulation depends on configuration or capability of computer system, type of modelling dimensions (1D, 2D or 3D), number of mesh and type of mesh elements, number of degrees of freedom, and also, complexity of modelling method (B-dependent model, anisotropic model, or simplified models). In Fig.12, the computation time of simulations to investigate the effect of nonsinusoidal carrying current on the AC transport current loss

has been shown in 3D plain view for all simulations in both cases of B-independent J_c and B-dependent with $B_0 = 125$ mT. It can be concluded from Fig.12 that in case of nonsinusoidal carrying current, the B-independent J_c modelling is about 15% faster than B-dependent modelling.

Now, checking the content of Table III shows that eventually, even a little amount of amplitude increase caused by harmonics could increase AC loss, drastically. In addition, it shows that THD is a better measure to show the effect of harmonics on AC loss increment.

IV. A CASE STUDY ON AC LOSS OF HTS POWER TRANSFORMERS USING A SEMI-ANALYTICAL METHOD: CONSIDERING HARMONIC SPECTRUM OF THE POWER NETWORK

The power transformers are one of the most important and most expensive equipments in power network, which their reliable performance and operation is absolutely vital for whole network reliability and power quality. In modern electrical networks, power transformers usually face with nonsinusoidal current or loads [25-28, 44]. Since the electrical networks are three-phase, some of the transformers have star-delta or star-neutral-star connections in primary or secondary windings, then no 3rd order of current harmonic can pass through the windings. In the real power network, the most important harmonic orders are odd harmonics with the order less than 11, especially 5th and 7th harmonic components [25-28]. Therefore, in this paper, these two orders have been considered for AC loss calculation of HTS transformer winding. For this purpose, nonsinusoidal currents with spectrum listed in Table V were applied to the HTS coil. Since, HTS transformer usually design to have overload capability of 50% to 100% of rated power, as one of their most important advantages compared with conventional oil-immersed transformers, so the fraction of transport current to critical current must be 50% or less to cover the overload requirements. As it is depicted in Fig.11, AC transport current loss increases very fast in higher THDs and higher carrying current close to I_c and since the nonsinusoidal currents contain a wide spectrum of different harmonic orders specially in polluted modern power networks, a safety margin must be considered between the operating carrying current of fundamental harmonic and the I_c of the tape or coil in the transformer; otherwise if HTS power transformers are designed to work in high (I/I_c) regime, then any changes in harmonic distortion of transformer load current may drive the tapes to shared superconductor-normal metal state situation which is very dangerous for the tapes and they are likely to burn in this mode. Therefore, when engineers design an HTS coil for an electrical machine e.g. HTS power transformer which will work in nonsinusoidal operating environment, they must use tapes with higher critical current in order to produce coils with higher critical current density and lower (I/I_c) factor to keep a reasonable safety margin in case any harmonics exist.

The distorted current waveforms with 5th and 7th harmonic contents were depicted in Fig.13 and compared with sinusoidal current. These nonsinusoidal currents with this specific harmonic spectrum which contains 5th and 7th orders are very common in electrical power networks and usually are produced by the nonlinear loads of industrial factories and distortions of compact fluorescent lamp in urban customers [45-46]. Theses nonsinusoidal currents have been applied as carrying current with 50% loading to the modeled HTS coil in COMSOL Multiphysics.

The AC transport current losses of the HTS coil versus THDs at 50% carrying current and 50 Hz fundamental frequency in both sinusoidal and nonsinusoidal cases have been shown in Fig.14. The simulation results show that for the considered spectrum for nonsinusoidal current, AC transport current loss increases by a power law versus THD of distorted current. The AC loss increase slows down in higher THDs, it is because of a phenomenon so-called “harmonic compensation effect”, which means the THDs as well as power loss decrease by more harmonic contents. This phenomenon is often useful for power system stability and means more harmonic contents would not always lead to higher losses. It happens because different harmonic orders possess different ups and downs in their wave-shape. While when we add several harmonic orders together, one harmonic ups can sit on another downs and vice versa; therefore, it could lead to a smoother waveform, which causes lower loss.

TABLE V
HARMONIC CONTENTS OF NONSINUSOIDAL CURRENTS FOR CASE STUDY OF HTS TRANSFORMER WINDING

Case No.	(h_1) %	$\left(\frac{h_5}{h_1}\right)$ %	$\left(\frac{h_7}{h_1}\right)$ %	THD (%)
1	100	0	0	0
2	100	10	10	14
3	100	20	10	23
4	100	30	20	36
5	100	30	30	42
6	100	40	30	50
7	100	40	40	57

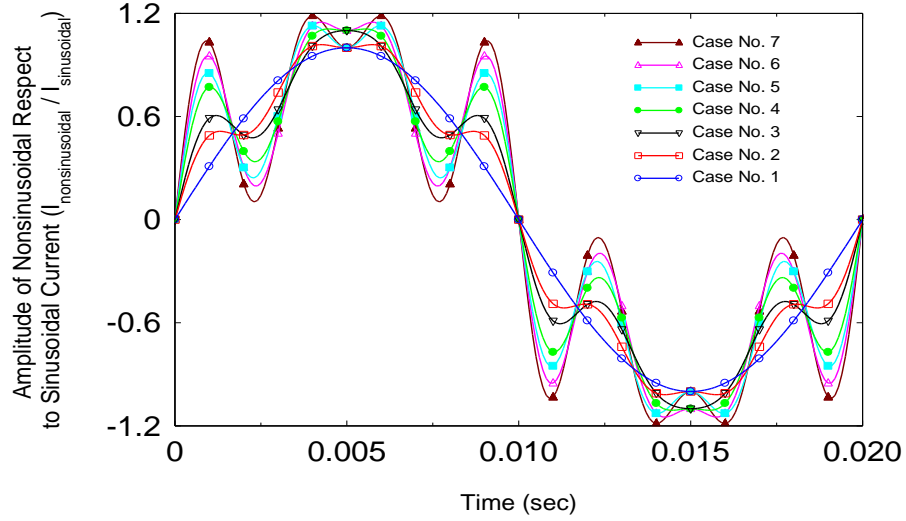


Fig. 13. The distorted current waveforms for HTS transformer case study at 50 Hz with 5th and 7th harmonic components

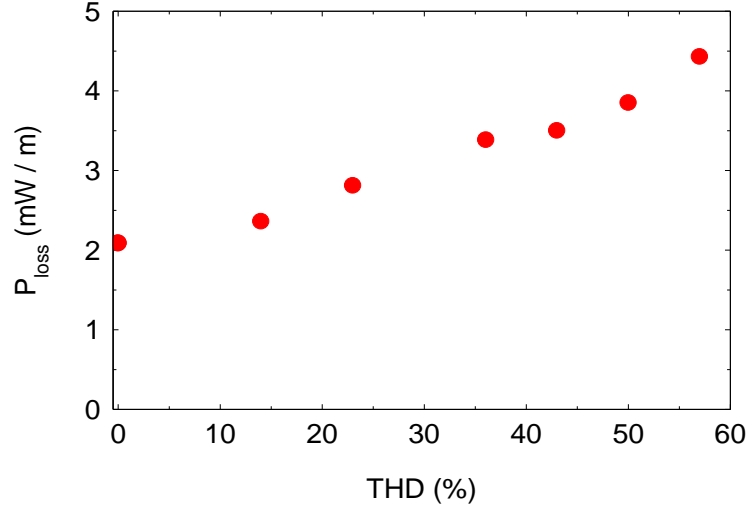


Fig. 14. The AC transport current loss versus THD at 50 Hz and 50% carrying current with 5th and 7th harmonic contents for HTS transformer case study

The relative increment of AC transport current loss of nonsinusoidal carrying current respect to sinusoidal one with a fitted power law were shown in Fig.15 along with the fit coefficient data. The fit formula is as follows:

$$(\text{Nonsinusoidal } P_{AC \text{ loss}}) = \alpha \times (\text{THD})^\beta \quad (14)$$

The power law coefficient (β) of this fit is in good agreement with the results of Table IV which was the curve fitting parameters for nonsinusoidal with only 5th harmonic content for short samples.

The fabrication and utilization of HTS transformers are economical for the apparent power more than 20MVA which is so-called HTS transformer breakeven power. In this paper for the case study, an HTS transformer with specifications tabulated in Table VI was considered. This 20MVA HTS power transformer was designed by YBCO windings with parameters which is listed in Table I. In this class of power transformers, voltage per turn (u) of the windings is about 100 Volt/turn. The diameter of the core can be calculated as follow [47]:

$$E_{ph} = V_p = 4.44 f k_{st} k_{pk} N_p B_{max} A_c \quad (15)$$

$$k = k_{st} k_{pk} \quad (16)$$

$$D_{core} = \sqrt{\frac{2\sqrt{2} u}{\pi^2 f k B_{core}^{max}}} \quad (17)$$

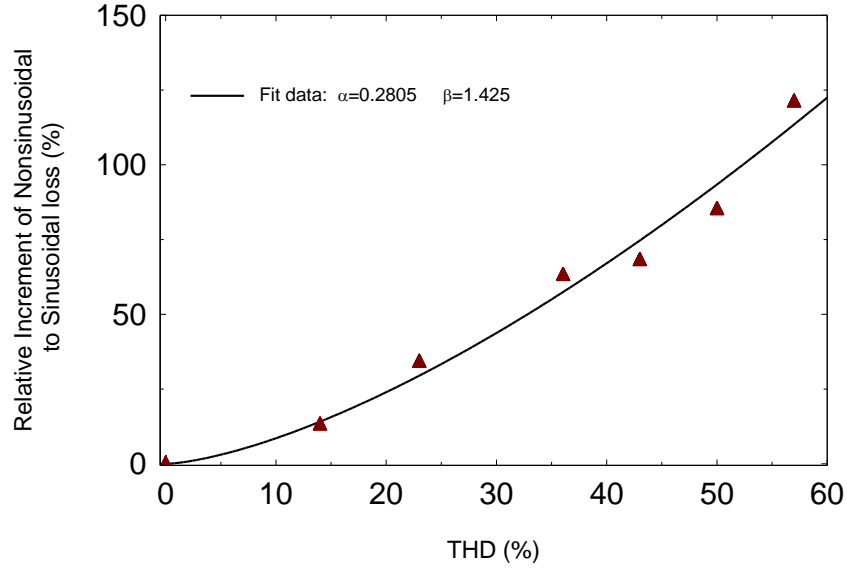


Fig. 15. Comparison between sinusoidal and nonsinusoidal AC transport current losses for HTS transformer case study at 50 Hz with 5th and 7th harmonic contents

TABLE VI
THE SPECIFICATIONS OF UNDER STUDIED HTS TRANSFORMER

Parameter	Value	Dimension
Apparent power	20	MVA
Fundamental frequency	50	Hz
Primary winding rated voltage	230	kV
Secondary winding rated voltage	64	kV
Winding connections	YnD	---

Where E_{ph} , k_{st} , k_{pk} , B_{max} , and A_c are phase induced voltage, stacking factor of core laminations, packing factor of core limb, maximum flux density in the core, and cross section area of core limb, respectively. D_{core} is diameter of the leg of the transformer core, and B_{core}^{max} is maximum flux density in the core.

The maximum parallel and perpendicular flux densities occur at the middle, and two ends of coils, respectively [47].

$$B_{\parallel}^{max} = \mu_0 \frac{\sqrt{2} (N_p I_p)}{g l_{coil}} \quad (18)$$

$$B_{\perp}^{max} = \mu_0 \frac{(N_p I_p)}{\sqrt{2} \pi g l_{coil}} \ln\left(\frac{2 l_{coil}}{w_{tape}}\right) \quad (19)$$

Where g , l_{coil} , and w_{tape} are number of groups of balanced ampere-turns in windings, length of the coil, and width of superconducting tape, respectively. N_p , w_{tape} , and I_p are number of turns in primary winding, superconducting tape width, and primary phase rated current, respectively.

Assuming the transformer parameters as such listed in Table VII, and considering 2 parallel paths for both primary and secondary, then the total length of the tape in primary and secondary windings are known.

One of the vital factors in cryogenic system design is accurate estimation of the energy dissipation in the form of AC loss in the HTS coils subjected to alternating currents. For example, in superconducting transformer applications, it is crucial to know the AC transport current loss of the windings accurately because the cryocooler must be able to dissipate the losses out of the cryostat optimally, which means the rating of cooling system and its penalty factor for dissipating the heat load out of cryostat are key factors to be considered in design stage; otherwise, these losses and the resultant generated heat increase and

as a consequence, the total efficiency of whole system including transformer and cooling part will decrease [8, 48]. As we know, there are two commonly used type of cryocoolers for superconducting transformers, i.e. Gifford-McMahon (GM), and Stirling systems. The most plausible cryocooler options from these two groups for such a large HTS transformer are Cryomech AL600 or Stirling SPC-4. Their nominal cooling penalty factors are 26 and 16, respectively. In case of GM cryocoolers, multiple unites are needed to dissipate the total amount of AC loss out of the cryostat [49]. Therefore, one can argue that the final total penalty factor would be even higher than these numbers. But in this paper, we only consider the optimistic scenario. Assuming optimistic penalty factor of the 20 for the cryocooler and cooling system of this HTS transformer to dissipate 1W of heat load out of its cryostat, then the heat load of cryocooler increases significantly in nonsinusoidal case compared with the heat load of sinusoidal situation i.e. the cryocooler will see a huge amount of extra heat load to dissipate out of cryostat which finally leads to total efficiency reduction of whole transformer and cooling system, together.

TABLE VII
THE ASSUMED PARAMETERS FOR CALCULATION OF HTS TRANSFORMER CASE STUDY

Parameter	Value	Dimension
k	0.85	---
u	100	V/turn
B_{core}^{max}	1.75	T
Overload rate	50	%
Number of parallel paths in primary and secondary	2	---
Cooling penalty factor	20	W/W

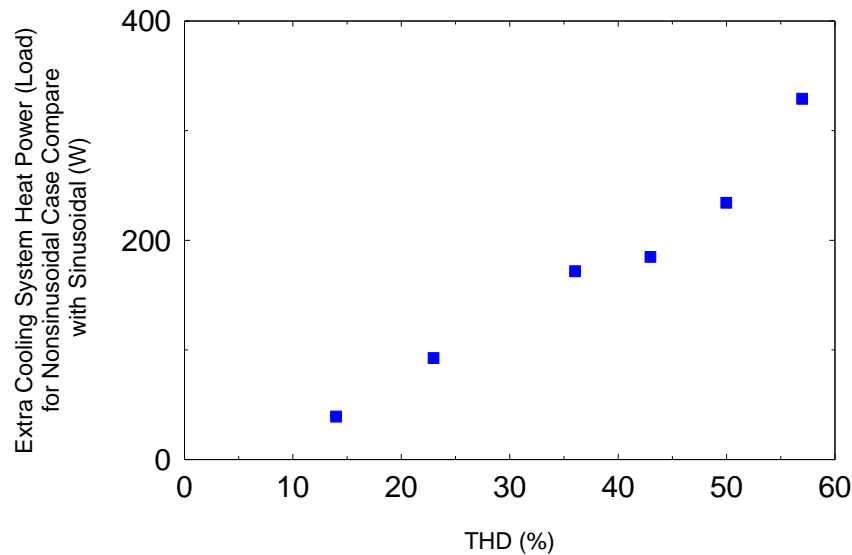


Fig. 16. Extra Heat load of cooling system versus THDs for HTS transformer case study at 50 Hz with 5th and 7th harmonic contents

The extra heat load or extra required cooling power which should be provided by cooling system of HTS power transformer versus THD of distorted current was shown in Fig. 16. When THD is around 10%, the extra power is about 50W and when THD=35%, this extra heat load is about 250W, which is significantly higher than normal sinusoidal operation of the HTS power transformer in non-polluted environment. Assuming a typical heat load around 1.5 kW for a 20 MVA HTS power transformer, it means that 10%, and 35% of THD in nonsinusoidal current leads to 3% and 15% extra heat load for transformer cooling system. The level of this extra heat load is proportional to the cooling penalty factor, i.e. higher penalty factor leads to higher heat load caused by AC loss. These values would be higher if one considers over-load situation. On the other hand, this extra heat load caused by nonsinusoidal AC loss may eventually increase the cost, weight, and occupied room of the HTS power transformer, because the GM cryocoolers usually come in discrete ratings, therefore any extra heat load may mean a need to a new stage of GM cryocooler which actually means much higher cost.

It should be mentioned that this extra imposed heat load to cryocooler is only and only because of the AC loss of HTS coil

in the winding; in other words, it is assumed that the heat load of cooling system is only governed by AC loss; but in reality there are some other elements contributing in total heat load of the cooling system such as heat leak, current lead heat load, fan load, and etc., which will increase these numbers, even much more drastically. Therefore, this heat load calculation is optimistic evaluation and harmonic will lead to even worse situation for cooling system. Some of other considerations for cooling system under this situation are type of cryocooler, number of cryocooler stages, allowable operating temperature range, working in subcooled or saturated vapor pressure situation, degree of subcooling, heat transfer performance of tape, coil, and windings, thermal specifications of impregnation material, precision of heat load estimation, level and period of operation under over-load condition, and etc.

Comparisons have been done on variation of flux density magnitude and variation of current density across the height of a single turn of HTS coil for HTS transformer. These comparison for B_{norm} and J_{HTS} were shown in Fig. 17 and performed between sinusoidal and nonsinusoidal currents at THD=23%, 50 Hz, 50% of carrying current level, $B_0=125mT$ in $\omega t=3\pi/4=120^\circ$. It can be seen from both figures that both parameters are varying in the height of the HTS coil, and are higher in ends which agree with theoretical knowledge.

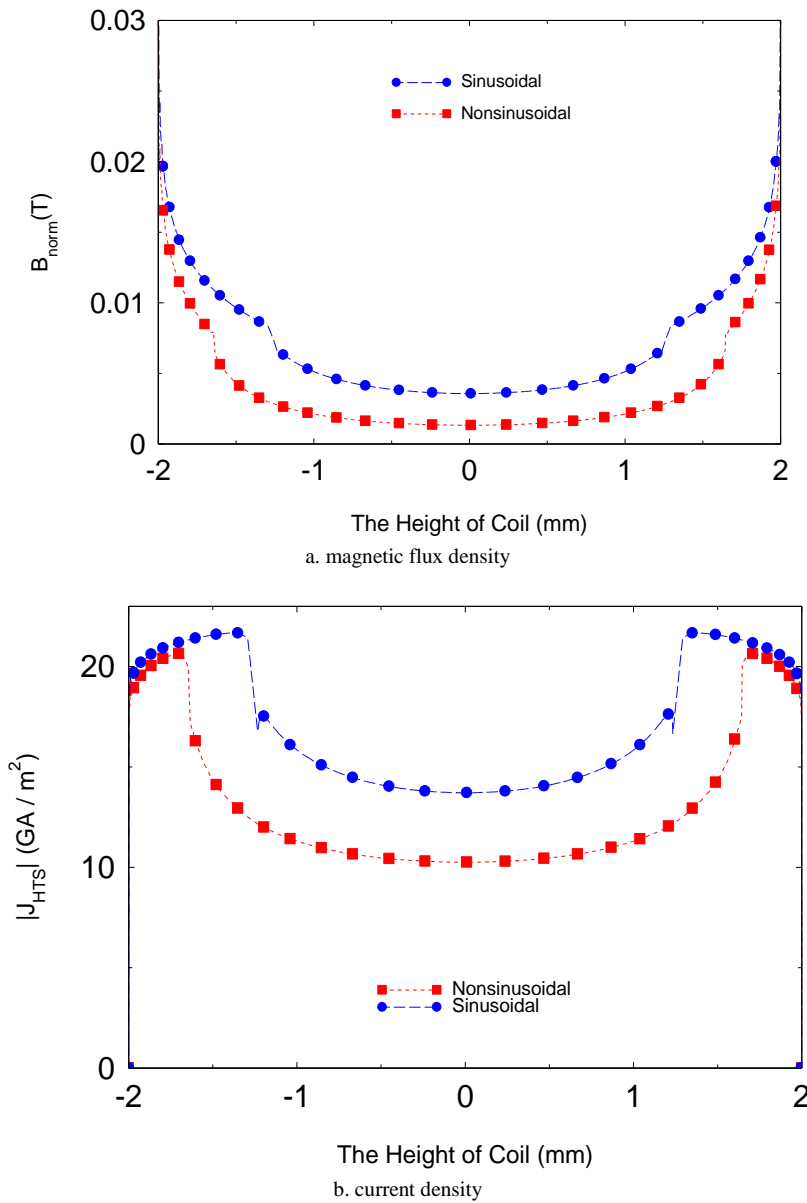


Fig. 17. Comparison between magnetic flux density and current density along the height of the HTS coil in sinusoidal and Case 3 of nonsinusoidal carrying current with 23% THD for HTS transformer case study at 50 Hz, 50% load and $B_0=125$ mT at $\omega t=3\pi/4$

V. CONCLUSION

In this paper, AC transport current losses of a single-turn 2G HTS coil were calculated using 2D numerical FE modelling approach based on H-formulation under sinusoidal and nonsinusoidal carrying currents. The effect of B-dependent critical current density on AC losses of an HTS power transformer carrying non-linear loads with different harmonic orders and THDs were studied. In order to compare AC transport current losses under sinusoidal and nonsinusoidal carrying currents, some FE simulations have been done in COMSOL Multiphysics as case studies on a superpower HTS tape with different carrying current amplitude respect to critical current (I/I_c), different fundamental frequency (f_1), different harmonic content, THD, and different magnetic field dependency factor of critical current density (B_0).

The AC transport current losses of the HTS coil is bigger in higher carrying current and higher frequencies, while it increases nonlinearly with current and frequency. In addition, when B-dependency of J_c is considered in simulations, the AC transport current loss is higher than B-independent J_c .

As for computation time, for B-dependent modelling the simulation time is 15% to 20% higher than B-independent J_c model. In addition, by increase of carrying current from 25% to 95% of critical current, the computation time of simulation increased by 4times.

The combinational harmonic orders of 5th and 7th harmonic were considered for a 20MVA HTS power transformer. In these simulations, the variation of nonsinusoidal AC transport current loss were varied by power law versus THDs. This loss increase leads to huge heat load increment for cryocooler and cooling systems of the HTS transformer and as a consequence, the total efficiency of the HTS transformer drops, significantly.

REFERENCES

- [1] S. S. Kalsi, "Applications of High Temperature Superconductors to Electric Power Equipment", John Wiley & Sons, Inc., USA, 2011.
- [2] M. Yazdani-Asrami, M. Staines, G. Sidorov, M. Davies, J. Bailey, N. Allpress, N. Glasson, and S. A. Gholamian, "Fault current limiting HTS transformer with extended fault withstand time," *Superconductor Science and Technology*, vol. 32, no. 3, 2019, pp. 1–13.
- [3] M. P. Staines, Z. Jiang, N. Glasson, R. G. Buckley, M. Pannu, "High-temperature superconducting (HTS) transformers for power grid applications", *Woodhead Publishing Series in Energy*, 2015, pp. 367–397.
- [4] B. G. Marchionini, Y. Yamada, L. Martini, and H. Ohsaki, "High Temperature Superconductivity: A Roadmap for Electric Power Sector Applications, 2015-2030", *IEEE Transactions on Applied Superconductivity*, vol. 27, no. 4, 2017, pp. 1-6.
- [5] M. Noe, and M. Steurer, "High-temperature superconductor fault current limiters: concepts, applications, and development status", *Superconductor Science and Technology*, vol. 20, 2007, pp. 15-29.
- [6] W. Song, J. Fang, Z. Jiang, M. Staines and R. Badcock, "AC Loss Effect of High-Order Harmonic Currents in a Single-Phase 6.5 MVA HTS Traction Transformer", *IEEE Transactions on Applied Superconductivity*, vol. 29, no. 5, 2019, pp. 1-5.
- [7] A. Berger, S. Cherevatskiy, M. Noe, and T. Leibfried, "Comparison of the Efficiency of Superconducting and Conventional Transformers", *Journal of Physics: Conference Series*, vol. 234, 2010, pp. 1-8.
- [8] W. Song, Z. Jiang, M. Staines, R. A. Badcock, S. Wimbush, J. Fang, and J. Zhang, "Design of a single-phase 6.5 MVA/25 kV superconducting traction transformer for the Chinese Fuxing high-speed train", *International Journal of Electrical Power & Energy Systems*, vol. 119, 2020, pp. 1-10.
- [9] M. Zhang, W. Yuan, J. Kvitkovic, and S. Pamidi, "Total AC loss study of 2G HTS coils for fully HTS machine applications", *Superconductor Science and Technology*, vol. 28, 2015, pp. 1-8.
- [10] W. Song, Z. Jiang, X. Zhang, M. Staines, R. Badcock, J. Fang, Y. Sogabe, and N. Amemiya, "AC loss simulation in a HTS 3-Phase 1 MVA transformer using H formulation," *Cryogenics*, vol. 94, 2018, pp. 14-21.
- [11] W. Li, H. Ye, J. Sheng, J. Jiang, B. Shen, Z. Li, Z. Hong, and Z. Jin, "Performance Evaluation of Conductor on Round Core Cables Used in High Capacity Superconducting Transformers", *IEEE Transactions on Applied Superconductivity*, vol. 30, no. 4, 2020, pp. 1-5.
- [12] R. Soman, H. Ravindra, X. Huang, K. Schoder, M. Steurer, W. Yuan, M. Zhang, S. Venuturumilli, and X. Chen, "Preliminary Investigation on Economic Aspects of Superconducting Magnetic Energy Storage (SMES) Systems and High-Temperature Superconducting (HTS) Transformers", *IEEE Transactions on Applied Superconductivity*, vol. 28, no. 4, 2018, pp. 1-5.
- [13] E. Pardo, M. Staines, Z. Jiang, and N. Glasson, "AC loss modelling and measurement of superconducting transformers with coated-conductor Roebel-cable in low-voltage winding" *Superconductor Science and Technology*, vol. 28, no. 11, 2015, pp. 1-19.
- [14] W. Song, Z. Jiang, M. Staines, S. Wimbush, R. Badcock, and J. Fang, "AC loss calculation on a 6.5 MVA/25 kV HTS traction transformer with hybrid winding structure", *IEEE Transactions on Applied Superconductivity*, Early Access, 2020.
- [15] F. Grilli, "Numerical Modeling of HTS Applications", *IEEE Transactions on Applied Superconductivity*, vol. 26, no. 3, 2016, pp. 1-8.
- [16] A. Morandi, "2D electromagnetic modelling of superconductors", *Superconductor Science and Technology*, vol. 25, 2012, pp. 1-22.
- [17] Z. Hong, L. Ye, M. Majoros, A. M. Campbell, and T. A. Coombs, "Numerical Estimation of AC Loss in MgB2 Wires in Self-field Condition", *Journal of Superconductivity and Novel Magnetism*, vol. 21, no.3, 2008, pp. 205-2011.
- [18] A. Stenvall, V. Lahtinen and M. Lyly, "An H-formulation-based three-dimensional hysteresis loss modelling tool in a simulation including time varying applied field and transport current: the fundamental problem and its solution", *Superconductor Science and Technology*, vol. 27, 2014, pp. 1-7.
- [19] R. Brambilla, F. Grilli, L. Martini, and F. Sirois, "Integral equations for the current density in thin conductors and their solution by the finite-element method", *Superconductor Science and Technology*, vol. 21, 2008, pp. 1-8.
- [20] M. D. Ainslie, W. Yuan, Z. Hong, R. Pei, T. J. Flack, and T. A. Coombs, "Modeling and Electrical Measurement of Transport AC Loss in HTS-Based Superconducting Coils for Electric Machines", *IEEE Transactions on Applied Superconductivity*, vol. 21, no. 3, 2011, pp. 3265-3268.
- [21] M. D. Ainslie, D. Hu, J. Zou, and D. A. Cardwell, "Simulating the In-Field AC and DC Performance of High-Temperature Superconducting Coils", *IEEE Transactions on Applied Superconductivity*, vol. 25, no. 3, 2015, pp. 1-5.
- [22] M. D. Ainslie, D. Hu, V. M. R. Zermeno, and F. Grilli, "Numerical Simulation of the Performance of High-Temperature Superconducting Coils", *Journal of Superconductivity and Novel Magnetism*, vol. 30, no.7, 2017, pp. 1987-1992.
- [23] F. Gomory, and J. Sheng, "Two methods of AC loss calculation in numerical modelling of superconducting coils, *Superconductor Science and Technology*", vol. 30, 2017, pp. 1-12.
- [24] M. Yazdani-Asrami, M. Mirzaie, and A. A. Shayegani Akmal, "No-load loss calculation of distribution transformers supplied by nonsinusoidal voltage using three-dimensional finite element analysis", *Energy*, vol. 50, 2013, pp. 205-2019.

- [25] M. Yazdani-Asrami, M. Mirzaie, and A. Akmal, "Investigation on Impact of Current Harmonic Contents on the Distribution Transformer Losses and Remaining Life" 2010 IEEE International Conference on Power and Energy (PECon 2010), pp. 689–694, 2010.
- [26] M. Mirzaie, M. Yazdani-Asrami, and A. Akmal, "Investigation of Load Loss Increase in Transformers Due to Harmonic Loads" Australian Journal of Electrical and Electronics Engineering, vol. 8, no. 3, pp. 247–255, 2011.
- [27] M. Mirzaie, M. Yazdani-Asrami, and A. Akmal, "Impacts of Non-Sinusoidal Load Currents on Distribution Transformer Losses-Part II: Standard Aspects and Experimental Measurement" International Review of Electrical Engineering, vol. 6, no. 5, pp. 2215–2220, 2011.
- [28] M. Mirzaie, M. Yazdani-Asrami, and A. Akmal, "Impacts of non-sinusoidal load currents on distribution transformer losses-Part I: Theoretical aspects and finite element based simulation" International Review of Electrical Engineering, vol. 6, no. 5, pp. 2207–2214, 2011.
- [29] R. Tebano, and F. Gomory, "Higher harmonics in the voltage on a superconducting wire carrying AC electrical current", Central European Journal of Physics, vol. 2, 2003, pp. 246-257.
- [30] G. Furman, M. Spektor, V. Meerovich, and V. Sokolovsky, "Losses in coated conductors under non-sinusoidal currents and magnetic fields", Journal of Superconductivity and Novel Magnetism, vol. 24, no.1-2, 2011, pp. 1045-1051.
- [31] V. Sokolovsky, V. Meerovich, M. Spektor, G. A. Levin, I. Vajda, "Losses in Superconductors under Non-Sinusoidal Currents and Magnetic Fields", IEEE Transactions on Applied Superconductivity, vol. 19, no. 3, 2009, pp. 3344-3347.
- [32] B. J. H. De Bruyn, J. W. Jansen, and E. A. Lomonova, "AC losses in HTS coils for high-frequency and non-sinusoidal currents", Superconductor Science and Technology", vol. 30, 2017, pp. 1-8.
- [33] B. Shen, C. Li, J. Geng, X. Zhang, J. Gawith, J. Ma, Y. Liu, F. Grilli, and T. A. Coombs, "Power dissipation in HTS coated conductor coils under the simultaneous action of AC and DC currents and fields," Superconductor Science and Technology, vol. 31, no. 7, pp. 1–12, 2018.
- [34] B. Shen, C. Li, J. Geng, Q. Dong, J. Ma, J. Gawith, K. Zhang, Z. Li, J. Chen, W. Zhou, X. Li, J. Sheng, Z. Li, Z. Huang, J. Yang, and T. A. Coombs, "Power Dissipation in the HTS Coated Conductor Tapes and Coils Under the Action of Different Oscillating Currents and Fields," IEEE Transactions in Applied Superconductivity, vol. 29, no. 5, pp. 1–5, 2019.
- [35] W. Song, J. Fang, and Z. Jiang, "Numerical AC Loss Analysis in HTS Stack Carrying Non-sinusoidal Transport Current," IEEE Transactions in Applied Superconductivity, vol. 29, no. 2, pp. 1–5, 2019.
- [36] M. Yazdani-Asrami, W. Song, X. Pei, M. Zhang, and W. Yuan, "AC Loss Characterization of HTS Pancake and Solenoid Coils Carrying Nonsinusoidal Currents," IEEE Transactions in Applied Superconductivity, vol. 30, no. 5, pp. 1–9, 2020.
- [37] G. R. Liu, and S. S. Quek, "The finite element method: a practical course", Elsevier Science Ltd., 2003.
- [38] V. M. Rodriguez-Zermeno, N. Mijatovic, C. Traholt, T. Zirngibl, E. Seiler, A. B. Abrahamsen, N. F. Pedersen, and M. P. Sorensen, "Towards Faster FEM Simulation of Thin Film Superconductors: A Multiscale Approach", IEEE Transactions on Applied Superconductivity, vol. 21, no. 3, 2011, pp. 3273-3276.
- [39] G. Messina, L. Morici, U. B. Vetrella, G. Celentano, M. Marchetti, P. Sabatino, and R. Viola, "AC Transport Current Losses in HTS Coils for Axial Flux Electrical Machines Applications", IEEE Transactions on Applied Superconductivity, vol. 24, no. 3, 2014, pp. 1-4.
- [40] M. Yazdani-Asrami, S. Asghar Gholamian, S. M. Mirimani, and J. Adabi, "Investigation on effect of magnetic field dependency coefficient of critical current density on the AC magnetizing loss in HTS tapes exposed to external field", Journal of Superconductivity and Novel Magnetism, vol. 31, no. 12, 2018, pp. 3899-3910.
- [41] B. Shen, F. Grilli, and T. Coombs, "Review of the AC loss computation for HTS using H formulation", Superconductor Science and Technology, vol. 33, no. 3, 2020, pp. 1-13.
- [42] G. K. Zhang, S. Hellmann, M. Calvi, and T. Schmidt, "Magnetization Simulation of Rebco Tape Stack with a Large Number of Layers Using the Ansys A-V-A Formulation", IEEE Transactions on Applied Superconductivity, vol. 30, no. 4, 2020, pp. 1-5.
- [43] F. Sass, G. G. Sotelo, R. de Andrade Junior, and F. Sirois, "H-formulation for simulating levitation forces acting on HTS bulks and stacks of 2G coated conductors", Superconductor Science and Technology, vol. 28, no. 12, 2015, pp. 1-12.
- [44] R. D. Henderson, and P. J. Rose, "Harmonics: The effects on power quality and transformers", IEEE Transactions on Industrial Applications, vol. 30, 1994, pp. 528-532.
- [45] L. Hocine, D. Yacine, B. Kamel, and K. M. Samira, "Improvement of electrical arc furnace operation with an appropriate model", Energy, vol. 34, no. 9, 2009, pp. 1207-1214.
- [46] C. H. Duarte, and R. Schaeffer, "Economic impacts of power electronics on electricity distribution systems", Energy, vol. 36, no. 1, 2011, pp. 520-529.
- [47] A. Morandi, L. Trevisani, P. L. Ribani, M. Fabbri, L. Martini, and M. Bocchi, "Superconducting transformers: key design aspects for power applications," Journal of Physics: Conference Series, vol. 97, no. 1, pp. 1–9, 2008.
- [48] S. R. Kim, J. Han, W. S. Kim, M. J. Park, S. W. Lee, and K. D. Choi, "Design of the Cryogenic System for 100 MVA HTS Transformer", IEEE Transactions on Applied Superconductivity, vol. 17, no. 2, 2007, pp. 1935-1938.
- [49] M. Staines, M. Yazdani-Asrami, N. Glasson, N. Allpress, L. Jolliffe, and E. Pardo, "Cooling systems for HTS transformers: impact of cost, overload, and fault current performance expectations", 2nd International Workshop on Cooling Systems for HTS Applications (IWC-HTS2017), vol. 1, 2017.